Geophys. J. Int. (1999) **138,** 353–365

A critique of frozen-flux inverse modelling of a nearly steady geodynamo

J. J. Love

School of Earth Sciences, University of Leeds, Leeds, LS2 9JT, *UK. E-mail: J.Love@earth.leeds.ac.uk*

Accepted 1999 March 3. Received 1999 February 8; in original form 1998 July 7

SUMMARY

Most inversions of geomagnetic secular variation for fluid flow at the core's surface utilize the so-called frozen-flux approximation where diffusion of the magnetic field is neglected. Here we note that the frozen-flux approximation can fail miserably for the geophysically relevant case of a nearly steady dynamo. We draw this conclusion from an inspection of the induction equation, after expanding the velocity and magnetic fields in terms of temporal mean and fluctuating parts (as is standard in mean-field electrodynamics). The resulting pair of equations, one describing steady dynamo action and the other describing secular variation, are coupled, and since steady dynamo action relies on diffusion, secular variation cannot be approximately described by the (diffusive-free) frozen-flux approximation. In support of this conclusion we present two new kinematic dynamo models. The first dynamo exhibits no secular variation even though it has a non-zero surface flow; for this dynamo no purely poloidal surface flow model can be constructed by using the frozen-flux approximation, but the actual surface flow is purely poloidal. The second dynamo exhibits westward drift of the magnetic field but has surface flow that is eastwards. Both of these models have magnetic Reynolds numbers much greater than unity, and so satisfy the criterion usually invoked for justifying the use of the frozen-flux approximation, and yet both of these models are contradictory to the frozen-flux approximation. Thus, inversions for core flow should consider the effects of diffusion. Core flow models deduced assuming that the frozen-flux approximation is valid, and any results dependent on such flow models, should be treated with a great deal of caution.

Key words: core flow, dynamo theory, geomagnetic field, geomagnetic secular variation.

INTRODUCTION

The Earth's magnetic field, sustained by dynamo action in the fluid core, changes over a wide range of timescales, from decadal variation detectable by historical measurements to occasional reversals and excursions seen in the geological record. However, despite its evident variability, outside of transitional periods most of the Earth's field consists of a persistent steady component, seen in both modern and palaeomagnetic data. In light of these observations, here we discuss some of the implications for the frozen-flux inverse modelling of a nearly steady geodynamo.

It was Halley (1692) who first surmised that secular variation of the magnetic field could be due to motion in the Earth's interior. Today, inverse theory is applied to historical observations of the Earth's magnetic field **B** in an attempt to deduce the fluid motion **u** at the core's surface. The starting point for such inversions is the induction equation,

$$\partial_t \mathbf{B} = \nabla \times (\mathbf{u} \times \mathbf{B}) + \eta \nabla^2 \mathbf{B} . \tag{1}$$

The left-hand side of this equation represents the secular variation; the terms on the right-hand side describe the effects of advection and diffusion, where η is the diffusivity. The relative sizes of the advective and diffusive terms are usually estimated by the magnetic Reynolds number,

$$R_{\mathrm{m}} = \frac{UL}{\eta} ; \tag{2}$$

U and L are characteristic velocities and length scales for the core, being estimated, respectively, from the rate of westward drift and as (say) the core radius. From a slightly different perspective, the magnetic Reynolds number can be

defined as the ratio of the characteristic diffusive timescale, τ_d, approximately that of a dipole, to the characteristic advective timescale, τ_a, approximately that of a convective overturn:

$$R_m = \frac{\tau_d}{\tau_a} . \tag{3}$$

With typical values one finds that $R_m \simeq 100$; in other words, advection is apparently more important than diffusion in governing the time dependence of the core's magnetic field.

Under such conditions, Alfvén (1942) proposed that diffusion could be neglected altogether, the magnetic field being effectively frozen into the fluid and governed by the reduced equation

$$\partial_t \mathbf{B} = \nabla \times (\mathbf{u} \times \mathbf{B}) . \tag{4}$$

In a geophysical context, Roberts & Scott (1965) suggested that this frozen-flux equation could be inverted for the (horizontal) flow at the core surface. A difficulty with including diffusion in an inversion for core flow is that the radial derivatives of the magnetic field on the core side of the core–mantle boundary (CMB) are unknown; neglecting diffusion makes the inversion more mathematically tractable. Many investigators have considered conditions under which the frozen-flux approximation might be applied (Backus 1968; Hide & Stewartson 1972; Braginsky & LeMouël 1993), and since Roberts & Scott's paper, other investigators have estimated core flow using the frozen-flux approximation (Kahle *et al.* 1967; LeMouël *et al.* 1985; Voorhies 1986; Bloxham 1988; Whaler & Clarke 1988; Lloyd & Gubbins 1990; Jackson & Bloxham 1991); see Fig. 1.

Although occasional hesitation has been expressed about the validity of the frozen-flux approximation (Bloxham & Gubbins 1986), the emphasis of the discussion has tended to be towards justification of the approximation. Unfortunately, two important points have not received the attention they deserve. First, a large part of the Earth's magnetic field can be considered steady, or at least slowly varying, over periods of time greater than a diffusive timescale. To lowest order, this observation is true in that the non-transitional field is predominantly dipolar; with respect to higher-order components, it has been suggested that stationary non-dipolar structure could be symptomatic of some form of core–mantle coupling (Hide 1967), with core flow locking onto mantle heterogeneities and thereby sustaining persistent magnetic field patterns. Second, many dynamo calculations using geophysically plausible flows sustain steady magnetic fields, even for very large magnetic Reynolds numbers (Kumar & Roberts 1975). These facts highlight the danger of the (simplistic) scaling arguments used in support of the frozen-flux approximation: over long periods of time the geodynamo is nearly steady even though the magnetic Reynolds number for the core is large. In other words, in the core the important balance in eq. (1) is not between secular variation and advection, but rather between advection and diffusion (their sum contributes almost nothing to the secular variation). Gubbins & Kelly (1996) have noted the inconsistency of inverting for steady core flow under the frozen-flux approximation, given the apparent reality of a nearly steady dynamo, and conclude that inversion of (4) is not always possible. Here we show that the problem with frozen flux becomes clear from a simple inspection of the mathematics and from examination of some new kinematic dynamos.

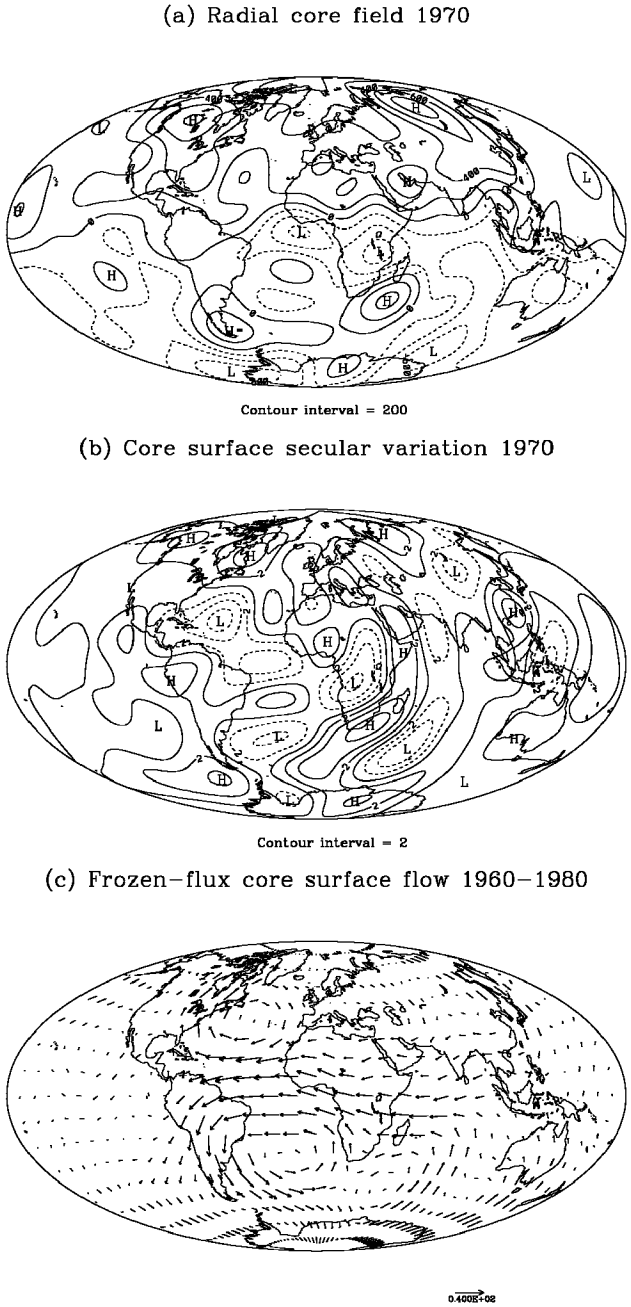

Figure 1. Radial component of the core field, B_r, its secular variation, $\partial_t B_r$, and a flow model, $\mathbf{u}_h$, determined by inversion under the frozen-flux approximation. (a) B_r (μT) for 1970 from the historical model of Bloxham & Jackson (1992). (b) $\partial_t B_r$ (μT yr^{-1}) for 1970 from the same model. (c) Steady $\mathbf{u}_h$ (km yr^{-1}) for 1960–1980 determined by Jackson & Bloxham (1991). All projections are Mollweide.

OBSERVATIONS

Before examining theoretical issues, it is instructive to compare statistically the palaeofield with the modern field. Towards that end, let us consider palaeomagnetic data covering the past 30 kyr, a duration which is comparable to the magnetic diffusive timescale of the whole core, but which is much longer than its convective overturn timescale ($\sim$300 yr). This period can be characterized as stable since the last well-defined transition is the Laschamp excursion, which occurred $\sim$40 kyr

Table 1. Summary of palaeomagnetic lava database. Each palaeomagnetic direction, inclination and declination (I, D), is an average of measurements from at least two magnetically cleaned samples per flow, with the precision parameter α_{95}, the semi-angle of the cone of 95 per cent confidence centred on the mean direction, less than 20°. Each absolute intensity datum (F) is an average of Thellier- or Shaw-type measurements, where the relative error σ_F/F is less than 33 per cent.

Locality	Name	Lat. (°N)	Long. (°E)	N	Age (kyr)	Author
France	Chaîne des Puys	45.7	3.0	6	1.7–12.0	Salis *et al.* (1989)
Hawaii	Hawaii	19.5	204.5	22	0.3–13.2	Mankinen & Champion (1993b)
Hawaii	Hawaii	19.5	204.5	6	13.5–31.1	Mankinen & Champion (1993a)
Hawaii	Hawaii	19.5	204.5	7	0.8–17.9	Coe *et al.* (1978)
Japan	Myoko, Fuji, Oshima, Sambe	36.0	138.5	6	3.0–6.0	Tanaka (1982)
Japan	Fuji, Oshima	35.5	138.7	6	9.0–13.7	Tanaka (1990)
Japan	Shikotsu	42.8	141.3	1	14.0	Tanaka *et al.* (1994)
Japan	Daisen	35.3	133.6	2	17.0–21.0	Tanaka *et al.* (1994)
Mexico	Chichinautzin	19.2	260.8	6	4.1–21.9	Gonzalez *et al.* (1997)
Mexico	Michoacan–Guanajuato	19.5	258.0	6	1.9–29.0	Gonzalez *et al.* (1997)
New Zealand	Taupo, Ruapehu	−38.9	175.8	2	9.9–22.0	Tanaka *et al.* (1994)
New Zealand	Whakapapa	−39.3	175.6	2	0.0–22.0	Tanaka *et al.* (1997)
Réunion	Remparts de Bellecombe	−21.1	55.5	9	4.8–11.0	Chauvin *et al.* (1991)
Sicily	Etna	37.6	15.0	22	0.0–0.8	Rolph & Shaw (1986)

ago (Roperch *et al.* 1988). In Table 1 and Fig. 2 we summarize a database of palaeomagnetic measurements (both directions and absolute intensities) taken from lava flows younger than 30 kyr at various sites around the world. Although this database is rather sparse, it is probably not temporally biased since volcanic activity is unrelated to, and therefore uncorrelated with, magnetic field variations. Moreover, since we consider only very recent lava depositions, we avoid bias due to palaeomagnetists' preference for sampling transitional periods (reversals and excursions); we have not discarded any data on the basis of arbitrary definitions distinguishing a transitional period from a stable period, such as latitude cut-off of virtual geomagnetic poles (VGPs). For the modern field we consider geographically and temporally uniformly distributed field vectors taken from the global model of Bloxham & Jackson (1992), a model which fits historical data covering the past 150 yr.

To compare intensity values (F) from different sites we normalize for site latitude λ:

$$F_{\mathrm{N}} = F(1+3\sin^2\lambda)^{-1/2}.$$

For directional data, inclination and declination (I, D), we measure the off-dipole angle δ, the angle between the magnetic vector and the local vector for an axial dipole field:

$$\cos\delta = \cos I_{\mathrm{AD}}\cos I\cos D + \sin I_{\mathrm{AD}}\sin I\,,$$

where

$$\tan I_{\mathrm{AD}} = 2\tan\lambda\,.$$

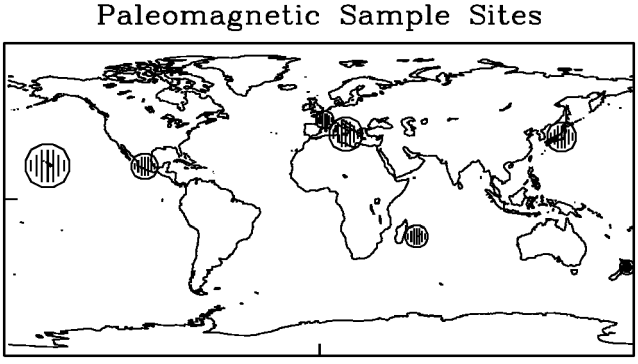

Figure 2. Geographic distribution of palaeomagnetic data sites; the size of the symbol is proportional to the number of data.

In Fig. 3 we compare the distributions of these quantities for both the palaeofield and the modern field. The normalized palaeointensity over the past 30 kyr is comparable to the modern value, being fairly constant at $\sim 33\ \mu$T; the variation about the mean value is relatively small, $\sigma_F < \overline{F}_{\mathrm{N}}$. With respect to the directions, the palaeomagnetic off-dipole angle is comparable to the modern value, $\overline{\delta} \simeq 12.5°$, indicating that the field over the past 30 kyr has resembled an axial dipole about as much as the field does today. In fact, Fig. 3 indicates that the palaeofield may actually have been on average slightly more dipolar than the modern field, but differences in the distributions may be due to the geographically sparse set of palaeomagnetic sample sites. In any case, in a statistical sense these data suggest that the main part of the non-transitional field is nearly steady and almost dipolar. This is, of course, not surprising; after all, the so-called geocentric axial dipole (GAD) hypothesis is of central importance to much palaeomagnetic research (Creer *et al.* 1954; Opdyke & Henry 1969).

Next, we examine the higher-order structure in the field's morphology (see also Yukutake & Tachinaka 1969; Bloxham & Gubbins 1985). In Fig. 4(a) we show the radial core field averaged over geological timescales (based on palaeomagnetic data) and in Fig. 4(b) the radial core field averaged over recent historical times. Gubbins & Kelly (1993) have remarked on their similarity: note, in particular, the coincidence of the flux patches underneath Canada and Siberia. In Fig. 4(c) we show the rms deviation from the historical time-averaged field. Note that the average deviation is much smaller than the mean itself. Of course, the 150 yr duration of the historical model covers a relatively brief period of secular variation, and is not sufficient by itself to draw conclusions about the long-term behaviour of the geomagnetic field. However, historical field models, together with the time-averaged palaeomagnetic

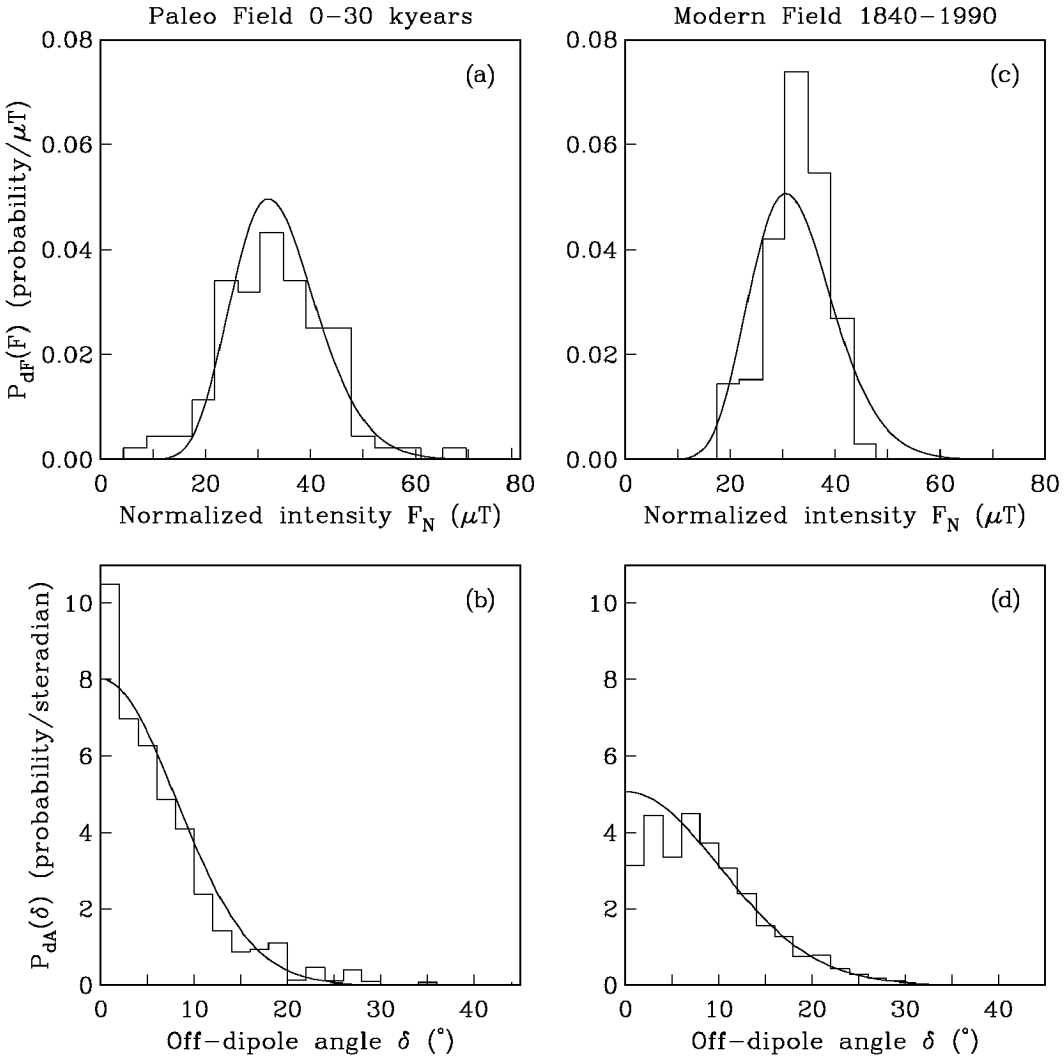

Figure 3. Statistical distributions of the geomagnetic field based on palaeomagnetic lava data covering the past 30 kyr and a random sampling of a modern field model covering the past 150 yr. On the top, the probability density functions of normalized intensity for (a) the palaeomagnetic data and (c) the modern field are shown. The histograms are based on binned data, the smooth curves are the best-fitting χ^2 distributions. For the palaeo (modern) field $\overline{F}_N \pm \sigma_F$ is 34.0 ± 10.9 μT (32.6 ± 5.8 μT). On the bottom, the probability density functions of off-dipole angle for (b) the palaeomagnetic data and (d) the modern field are shown. The histograms are based on binned data, the smooth curves are the best-fitting Fisher distributions. For the palaeo (modern) field $\overline{\delta} \pm \sigma_\delta$ is $12.4° \pm 9.4°$ ($12.8° \pm 6.2°$).

model, are consistent with the statistical results presented in Fig. 3, all of which suggest that, outside of transitional periods, the main part of the Earth's magnetic field is nearly steady over long, even geological, timescales. Time dependence applies to the smaller part of the field, being a perturbation superimposed upon a predominant steady field.

STEADY DYNAMO PLUS SECULAR VARIATION

We are motivated by these observations to describe the non-transitional geomagnetic field by expansions like those used in mean-field electrodynamics (Steenbeck *et al.* 1966):

$$\mathbf{B}(t) = \overline{\mathbf{B}} + \mathbf{B}'(t), \tag{5}$$

where $\overline{\mathbf{B}}$, being an average over time, is time-independent and $\mathbf{B}'$ is time-dependent with zero mean. For any analysis of secular variation over historical timescales, and probably longer, the mean field is typically larger than the fluctuating part, i.e. $\overline{B} > B'$. A similar expansion might be made for the flow as well,

$$\mathbf{u}(t) = \overline{\mathbf{u}} + \mathbf{u}'(t), \tag{6}$$

although it is not automatically clear that $\overline{u} > u'$; we do not make any assumption about the relative sizes of the time-averaged and time-dependent parts of the flow. For the purpose of the discussion that follows these mathematical expansions, similar to those made previously by Braginsky (1984) also in the context of secular variation, are hypothetical; in actuality we expect that it would be difficult to separate the mean magnetic field from the fluctuating field, and consequently even more difficult to invert for separate mean and fluctuating flows. To estimate accurately the mean magnetic field one would need data covering a period of time longer than the characteristic timescale of the secular variation, thus the historical data by themselves are probably insufficient. On the

other hand, palaeomagnetic data, although of lower quality than the historical data, cover a sufficient period of time to estimate a meaningful mean field. Technicalities such as these need to be addressed by those who seek to invert for core flow, which is not our intention here.

What are the kinematic implications for these expansions? Expansion of the magnetic field and flow into mean and fluctuating parts leads to a pair of equations

$$0=\nabla\times\overline{\boldsymbol{\mathcal{E}}}+\eta\nabla^2\overline{\mathbf{B}}\,, \tag{7}$$

$$\partial_t\mathbf{B}'=\nabla\times\boldsymbol{\mathcal{E}}'+\eta\nabla^2\mathbf{B}'\,, \tag{8}$$

where

$$\overline{\boldsymbol{\mathcal{E}}}=\overline{\mathbf{u}}\times\overline{\mathbf{B}}+\overline{\mathbf{u}'\times\mathbf{B}'}\,, \tag{9}$$

$$\boldsymbol{\mathcal{E}}'=\overline{\mathbf{u}}\times\mathbf{B}'+\mathbf{u}'\times\overline{\mathbf{B}}+\mathbf{u}'\times\mathbf{B}'-\overline{\mathbf{u}'\times\mathbf{B}'}\,. \tag{10}$$

(a) Paleomagnetic time averaged radial core field

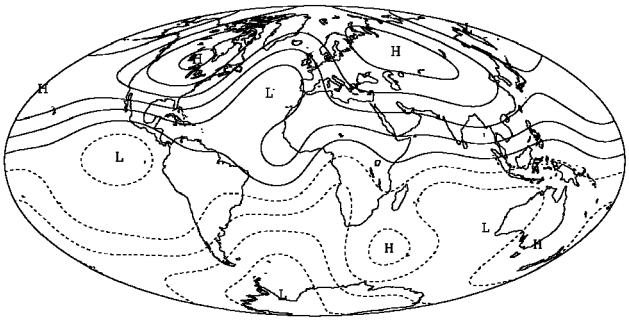

(b) Average radial core field 1840–1990

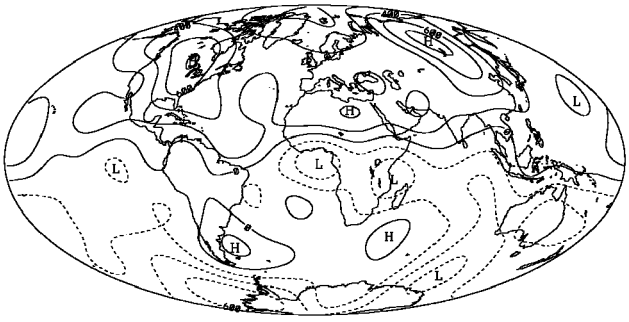

Contour interval = 200

(c) RMS deviation of radial core field 1840–1990

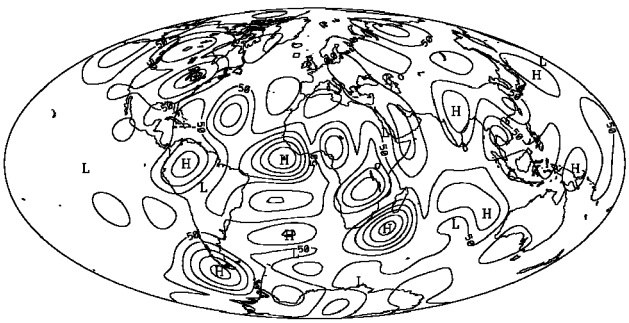

Contour interval = 50

Eq. (7), of course, describes time-averaged dynamo action; eq. (8) describes secular variation. In analysis of the secular variation, usually only the radial component of the field is used, in which case the relevant equations are

$$0=-\nabla\cdot\overline{\boldsymbol{\mathcal{E}}}_{\rm h}+\eta\nabla^2\overline{B}_{\rm r}\,, \tag{11}$$

$$\partial_t B'_{\rm r}=-\nabla_{\rm h}\cdot\boldsymbol{\mathcal{E}}'_{\rm h}+\eta\nabla^2 B'_{\rm r}\,, \tag{12}$$

where, in spherical coordinates (r, θ, ϕ), the subscript h denotes the tangential (horizontal) component, i.e. $\boldsymbol{\mathcal{E}}_{\rm h}=\boldsymbol{\mathcal{E}}-\mathscr{E}_{\rm r}\hat{r}=(0, \mathscr{E}_\theta, \mathscr{E}_\phi)$, and where

$$\overline{\boldsymbol{\mathcal{E}}}_{\rm h}=\overline{\mathbf{u}}_{\rm h}\overline{B}_{\rm r}+\overline{\mathbf{u}'_{\rm h}B'_{\rm r}}\,, \tag{13}$$

$$\boldsymbol{\mathcal{E}}'_{\rm h}=\overline{\mathbf{u}}_{\rm h}B'_{\rm r}+\mathbf{u}'_{\rm h}\overline{B}_{\rm r}+\mathbf{u}'_{\rm h}B'_{\rm r}-\overline{\mathbf{u}'_{\rm h}B'_{\rm r}}\,. \tag{14}$$

These apparently straightforward decompositions highlight the problem with justifying the frozen-flux approximation using length scale arguments. They are at variance with the scenario envisioned by some, such as by Braginsky (1991) and Hulot & LeMouël (1994), who suggest that diffusion is important in the maintenance of the large-scale, mostly dipolar main field but that the frozen-flux approximation describes the secular variation. In fact, since the advective term in the induction equation (1) is bilinear in $(\mathbf{u}, \mathbf{B})$, not linear, eqs (11) and (12) are coupled, meaning that a tidy distinction between dynamo action and secular variation is not possible.

In contrast to eqs (11) and (12), practitioners of inversion under the frozen-flux approximation are using

$$\partial_t B'_{\rm r}=-\nabla_{\rm h}\cdot(\overline{\boldsymbol{\mathcal{E}}}_{\rm h}+\boldsymbol{\mathcal{E}}'_{\rm h})\,. \tag{15}$$

An important difficulty should now be evident: neglecting diffusion in eq. (12) does not give eq. (15). There is an additional and erroneous advective term in (15), namely $\nabla_{\rm h}\cdot\overline{\boldsymbol{\mathcal{E}}}_{\rm h}$, that should be balanced by diffusion, as in the time-averaged dynamo equation (11). Instead, under the frozen-flux approximation $\nabla_{\rm h}\cdot\overline{\boldsymbol{\mathcal{E}}}_{\rm h}$ generates secular variation. The seriousness of this problem appears not to have been appreciated by the

Figure 4. Radial components of the core surface field, $B_{\rm r}$, and its variance. (a) Steady field from 2.5 Myr of palaeomagnetic data (Gubbins & Kelly 1993) (relative intensity). (b) 150 year time-averaged part of the historical field (Bloxham & Jackson 1992),

$$\overline{B}_{\rm r}=\frac{1}{T}\int_{t_{\rm s}}^{t_{\rm e}}B_{\rm r}dt\,,$$

where $T=t_{\rm e}-t_{\rm s}$ is the duration of the average. (c) rms deviation of the historical field from its time average,

$$\sigma(B_{\rm r})=\left[\frac{1}{T}\int_{t_{\rm s}}^{t_{\rm e}}[B_{\rm r}-\overline{B}_{\rm r}]^2dt\right]^{1/2}.$$

Note that the deviation is smaller in amplitude and has a shorter length scale then the time-averaged field. The rms average radial field strength is

$$\langle B_{\rm r}\rangle=\left[\frac{1}{4\pi T}\int_{t_{\rm s}}^{t_{\rm e}}\oint_{\rm CMB}B_{\rm r}^2dSdt\right]^{1/2}=321.6\ \mu{\rm T}\,,$$

whilst the rms deviation is

$$\langle B_{\rm r}-\langle B_{\rm r}\rangle\rangle=\left[\frac{1}{4\pi T}\int_{t_{\rm s}}^{t_{\rm e}}\oint_{\rm CMB}[B_{\rm r}-\langle B_{\rm r}\rangle]^2dSdt\right]^{1/2}=75.5\ \mu{\rm T}\,.$$

All projections are Mollweide.

geophysical community: the frozen-flux approximation, as it is now applied, can fail miserably for the geophysically relevant case of a nearly steady dynamo! The reason for this is due to the coupling of steady dynamo action and secular variation, together with the reliance of dynamo action on diffusion.

Depending on the relative sizes of the steady and fluctuating velocity components ($\overline{\mathbf{u}}$, $\mathbf{u}'$) and their geometric relationship to the magnetic field ($\overline{\mathbf{B}}$, $\mathbf{B}'$), is it possible that the steady advective term is negligible compared to the fluctuating advective term. In other words, at the core surface is

$$|\nabla_h \cdot \overline{\mathcal{E}}_h| \ll |\nabla_h \cdot \mathcal{E}'_h| ? \tag{16}$$

In particular, it might be suggested that this condition would be satisfied if the steady part of the field is primarily dipolar, g_1^0, and that the flow is, as commonly thought, primarily differential rotation, t_1^0 (Elsasser 1947). However, we recall that much of the expectation that toroidal flow is dominant comes from the observation of the westward drift itself (Bullard *et al.* 1950). Thus, appealing to observations of westward drift as evidence of primarily toroidal flow, then arguing that condition (16) is accurate, is little more than circular logic. Assuming that this condition is satisfied is, after all, contrary to the motivation of inverting for core flow in the first place: it is distasteful to invert for flow models that satisfy poorly motivated and rather odd *a priori* expectations, which is what (16) represents. It is very possible that models of core flow obtained under such assumptions would bear no resemblance to the actual core flow (and there would, of course, be no way of knowing for certain). Having said all of this, even if a condition like (16) could be justified, it would still be incumbent upon the practitioner of frozen-flux inversion to justify the assumption that $\eta\nabla^2 B'_r$ is negligible compared to the advective term $\nabla_h \cdot \mathcal{E}'_h$; this condition is not satisfied for dynamo 2 presented below.

Finally, it might be argued that it is reasonable to invert (4) if one considers data from a sufficiently short period of time (such as a historical timescale of a century or so), the thinking being that perhaps diffusion does not contribute much to the secular variation over short timescales. In our view such a philosophy represents a confusion of timescales: a justification for an inversion must be made using the timescale characterizing the physical phenomenon, not the timescale over which the phenomenon is observed (see also Braginsky 1984). Since the main part of the field is steady over geological timescales, $\overline{B} > B'$, an inversion for core flow which uses the main part of the field $\overline{\mathbf{B}}$ must accommodate the physics that comes into play over such timescales. The issue, once again, concerns not so much the relative contribution of advection and diffusion to the secular variation, but instead the rough balance between advection and diffusion; together these effects contribute almost nothing to the secular variation. This balance is determined by the core flow and sustains the main part of the field one would use in an inversion for that same flow. Simply using data covering a short period of time does not change the physics and does not make the difficulty of incorporating diffusion into an inverse problem go away.

DYNAMO MODELS

To clarify some of these issues it is instructive to examine kinematic dynamos; details of our calculations are given in the Appendix. In Fig. 5 we show results from a simple kinematic dynamo calculation (dynamo 1); both the field and the flow in this model are steady. Dynamo action occurs for a critical magnetic Reynolds number of ~ 79, and within the volume of the fluid there is a large amount of poloidal motion (see Table 2). The flow at the surface of this model consists of pairs of upwelling and downwelling centres arranged along the equator. However, despite the evident non-axisymmetric form of the surface flow, the magnetic field at the surface is highly axisymmetric, consisting basically of flux spots at the geographic poles. These results are contradictory to published expectations that centres of downwelling, particularly for $R_m \gg 1$, should correspond to flux spots (Parker 1963; Allan & Bullard 1966). Instead, for this dynamo, the surface magnetic field is a complicated product of advection (and diffusion!) distributed over the volume of the fluid; hidden below the surface and extending over the radius of the sphere there is some downwelling along the geographic poles, but this is only a minor part of the total flow. Clearly we should be careful about making simple interpretations of core surface flow based only on the observed magnetic field.

Since dynamo 1 is steady it exhibits no secular variation; advective amplification is balanced by diffusion even though the magnetic Reynolds number is relatively large. However, the practitioner of frozen-flux inversion would utilize the equation

$$0 = -\nabla_h \cdot [(\mathbf{u}_{||} + \mathbf{u}_{ts})\overline{B}_r]. \tag{17}$$

The flows recoverable from this equation are non-unique: they can be purely toroidal, $\mathbf{u}_{||}$, following contours of B_r (Roberts & Scott 1965), or they can be a mixture of toroidal and poloidal ingredients, $\mathbf{u}_{ts}$ (Backus 1968). However, for a steady magnetic field no flows recoverable under frozen-flux inversion can be purely poloidal (Madden & LeMouël 1982; Gire *et al.* 1986). Thus, since the actual surface flow $\mathbf{u}_h$ of this dynamo is purely poloidal, frozen-flux inversion is bound to fail. Furthermore, the reader may be interested to know that we have also found steady kinematic dynamos sustained by purely poloidal motions (no toroidal motion anywhere) similar to those found by Love & Gubbins (1996a) but with non-zero surface flow. Of

Table 2. Summary of dynamo models. (ω, α^0, α^s, α^c) are model parameters as defined in the Appendix. R_m^c is the critical magnetic Reynolds number at which dynamo action occurs. $\langle \mathbf{t}^2 \rangle$ and $\langle \mathbf{s}^2 \rangle$ are the percentages of toroidal and poloidal kinetic energies in the flow. $\langle \mathbf{T}^2 \rangle$ and $\langle \mathbf{S}^2 \rangle$ are the percentages of toroidal and poloidal magnetic energies in the field.

Dynamo	ω	α^0	α^s	α^c	R_m^c	$\langle \mathbf{t}^2 \rangle$ (%)	$\langle \mathbf{s}^2 \rangle$ (%)	$\langle \mathbf{T}^2 \rangle$ (%)	$\langle \mathbf{S}^2 \rangle$ (%)
1	−16.77	−4.19	0.84	0.84	67.59	38	62	67	33
2	2.15	2.15	0.54	0.54	151.91	81	19	85	15

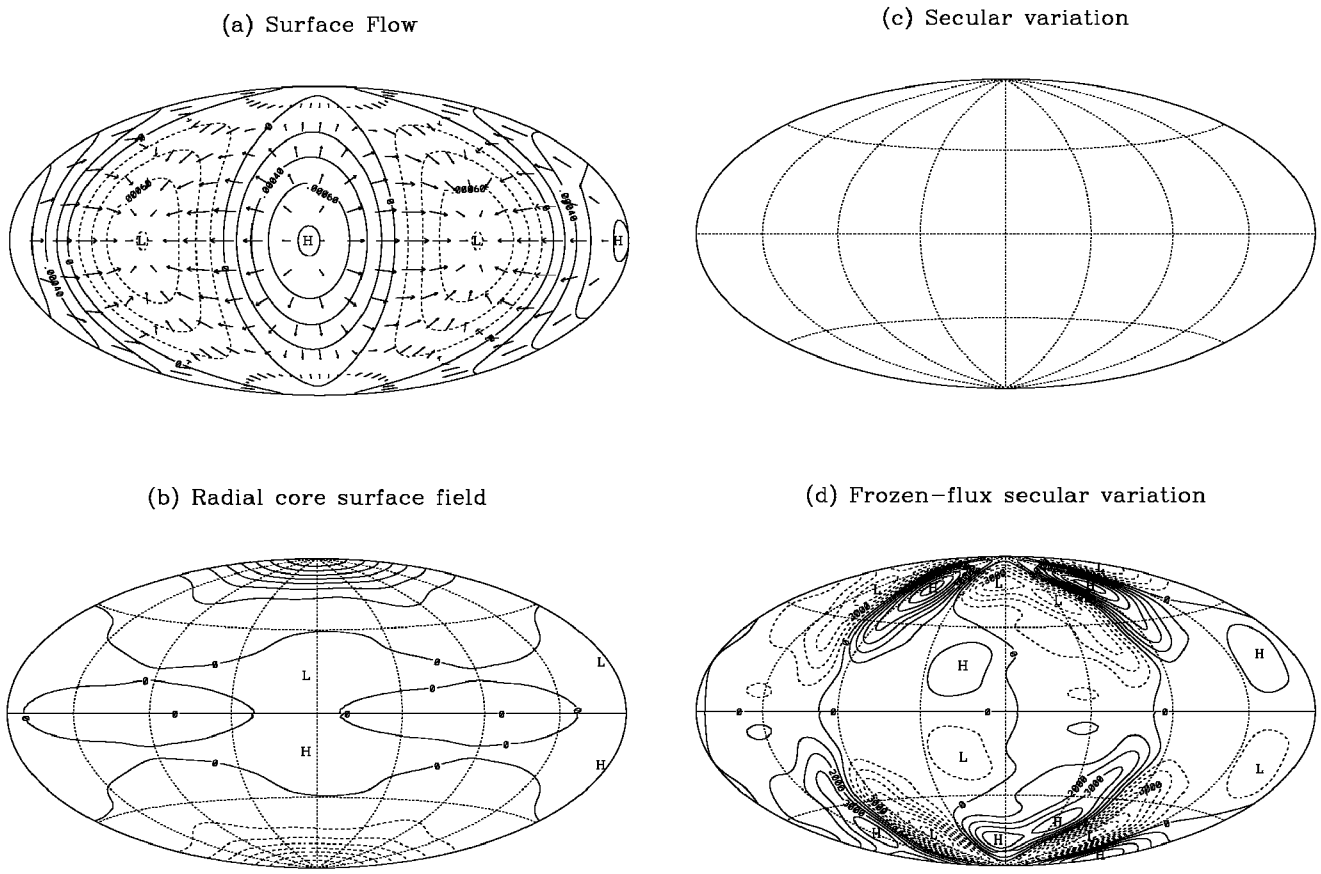

Figure 5. Surface characteristics of dynamo 1. (a) Surface flow, $\mathbf{u}_h$, which is purely poloidal and non-axisymmetric. (b) Radial component of the surface magnetic field, B_r, which is highly axisymmetric. (c) Secular variation, $\partial_t B_r$, which is identically zero due to a balance between advection and diffusion. (d) Secular variation for the actual surface flow if the frozen-flux approximation held (where diffusion is neglected). Units are arbitrary with the field normalized so that $g_1^0 = 1$. All projections are Mollweide.

course, frozen-flux inversion fails to determine the flows for these dynamos as well. In terms of the discussion in the previous section, condition (16) is not satisfied for these dynamos since at the surface $\nabla_h \cdot \overline{\mathcal{E}}_h = \nabla_h \cdot (\overline{\mathbf{u}}_h \overline{B}_r) \neq 0$ whilst $\nabla_h \cdot \mathcal{E}'_h = 0$. Finally, to look at the problem another way, in Fig. 5 we show the actual secular variation, which is zero, together with the expected secular variation for the actual surface flow but where the frozen-flux approximation held, namely

$$\partial_t B'_r = -\nabla_h \cdot (\overline{\mathbf{u}}_h \overline{B}_r) . \tag{18}$$

The frozen-flux secular variation is non-zero and therefore wrong.

As a second example, consider Fig. 6 (dynamo 2); neither the field nor the flow in this model are entirely steady, although parts of both are. The critical magnetic Reynolds number is ~ 150 and within the volume of the fluid the flow is primarily toroidal differential rotation (see Table 2); in contrast to the previous dynamo, here the flow at the surface is purely toroidal. However, despite the evident axisymmetric form of the surface flow, the magnetic field at the surface is noticeably non-axisymmetric, consisting basically of four symmetrically arranged flux spots. As with the previous dynamo, the surface magnetic field is a complicated product of advection and diffusion distributed over the volume of the fluid; hidden below the surface and extending over the radius of the sphere there is some non-axisymmetric poloidal motion. We are reminded that we need to be careful about making simple interpretations of core surface flow based only on the observed magnetic field. Dynamo 2 makes this point especially clearly since the non-axisymmetric parts of the magnetic field are steadily drifting west whilst the surface flow is steady and eastwards!

For the secular variation exhibited by dynamo 2, to determine a purely toroidal flow the practitioner of frozen-flux inversion would utilize the equation

$$\partial_t B'_r = -\nabla_h \cdot [(\overline{\mathbf{u}}_{||} + \mathbf{u}_w)(\overline{B}_r + B'_r)] . \tag{19}$$

The toroidal flows recoverable from this equation must contain a steady westward component $\overline{\mathbf{u}}_w$; the inversion is non-unique and the flow can have a component $\mathbf{u}_{||}$ following contours of B_r. Unfortunately, as with dynamo 1, what is absolutely impossible to determine under the frozen-flux approximation is the actual surface flow $\overline{\mathbf{u}}_h$ of this dynamo (here, steadily eastwards). Interestingly, in this case since the secular variation consists only of a steady westward drift, the time-averaged parts of the field (flow) are just the axisymmetric parts and the fluctuating parts of the field (flow) are just the non-axisymmetric parts; moreover, since the flow at the surface is axisymmetric, it is also steady there. Thus, in terms of the discussion in the previous section, condition (16) is satisfied for this dynamo since at the surface

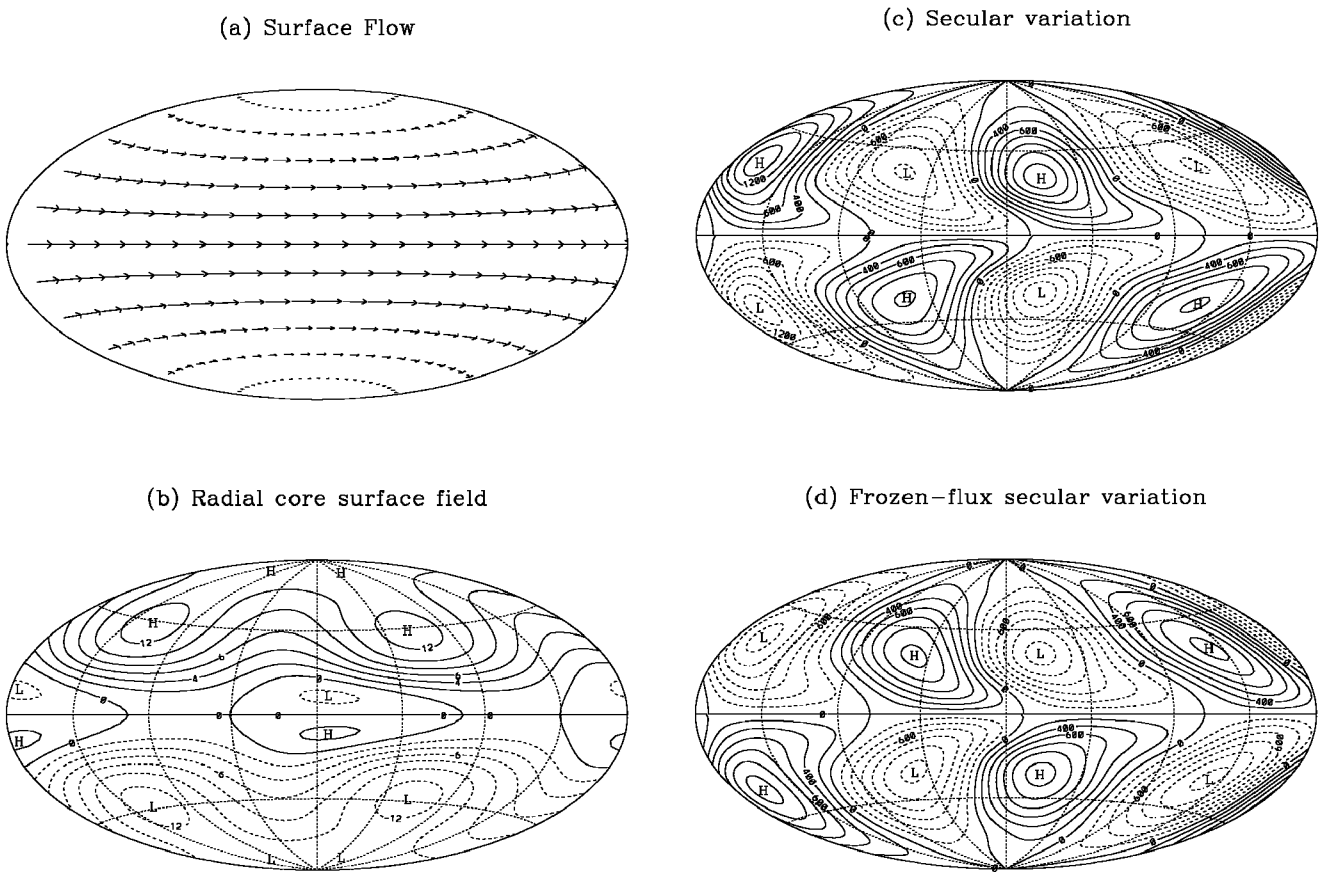

Figure 6. Surface characteristics of dynamo 2. (a) Surface flow, $\mathbf{u}_h$, which is purely toroidal, axisymmetric and progressing eastwards. (b) Radial component of the surface magnetic field, B_r, which has important non-axisymmetric ingredients that are steadily drifting west. (c) Secular variation, $\partial_t B_r$, due to a combination of advection and diffusion. (d) Secular variation for the actual surface flow if the frozen-flux approximation held (where diffusion is neglected); note that this is opposite to the actual secular variation. Units are arbitrary with the field normalized so that $g_1^0 = 1$. All projections are Mollweide.

$\nabla_h \cdot \overline{\mathcal{E}}_h = \nabla_h \cdot (\overline{\mathbf{u}}_h \overline{B}_r) = 0$, whilst $\nabla_h \cdot \mathcal{E}'_h \neq 0$. However, the frozen-flux approximation still fails, as can be seen in Fig. 6. Compare the actual secular variation, which at the fluid surface is determined by

$$\partial_t B'_r = -\nabla_h \cdot (\overline{\mathbf{u}}_h B'_r) + \eta \nabla^2 B'_r , \tag{20}$$

with the expected secular variation for the actual surface flow but where the frozen-flux approximation held, namely

$$\partial_t B'_r = -\nabla_h \cdot (\overline{\mathbf{u}}_h B'_r) . \tag{21}$$

The two quantities are exactly the opposite of each other! The difference is due solely to diffusion of the fluctuating part of the magnetic field B'_r (which some might have thought would be negligible).

It might be suggested that the velocity fields used in these dynamo calculations do not resemble that present in the Earth's core, or it might be suggested that we should be considering fully dynamic simulations. We admit that our discussion of kinematic dynamos has been highly idealized, we do not wish to ascribe undue attention to, nor do we hold unjustifiable faith in the geophysical verisimilitude of, individual details of our kinematic models. Our objective has been simply to illustrate that for the geophysically relevant case of a nearly steady dynamo, solutions to

$$\partial_t \mathbf{B} = \nabla \times (\mathbf{u} \times \mathbf{B}) + \eta \nabla^2 \mathbf{B} \tag{22}$$

do not in general resemble solutions to

$$\partial_t \mathbf{B} = \nabla \times (\mathbf{u} \times \mathbf{B}) , \tag{23}$$

even for the large magnetic Reynolds numbers usually invoked for justifying the frozen-flux approximation. Thus, having found that the frozen-flux approximation fails for simple dynamo models, it seems clear that there is reasonable doubt about its applicability to the reality of a much more complicated geomagnetic field.

CONCLUSIONS

Dropping diffusion from the induction equation changes its differential order, which can drastically affect the nature of any solution. This fact is particularly important to note when the basic state is nearly steady, as it is much of the time for the Earth. The induction equation is bilinear and thus expansion of the magnetic field and flow into mean and fluctuating parts leads to a pair of equations, one describing steady dynamo action and one describing secular variation. Because these equations are coupled, and since steady dynamo action relies on diffusion, the error in describing secular variation by the (diffusive-free) frozen-flux approximation may be nothing short of egregious. With the support of the dynamo calculations presented here we conclude that flow models deduced

assuming that the frozen-flux approximation is valid, and any results dependent on such flow models, should be treated with a great deal of caution.

Having found that the frozen-flux approximation can fail for the geophysically relevant case of a nearly steady dynamo, we are forced to conclude that inversions for core flow should consider the effects of diffusion. Voorhies (1993), Gubbins (1996) and Love & Gubbins (1996b) have all suggested kinematic methods for doing just that. Unfortunately, in practice this means a dramatic increase in the dimension of the model space, something that makes the analysis more difficult. However, since not all kinematic solutions are dynamically realizable, incorporation of dynamics may (at least ultimately) help to alleviate some of these difficulties by reducing the size of the permissible model space.

ACKNOWLEDGMENTS

We thank D. Gubbins, A. Jackson and G. Sarson for constructive conversations. We thank R. Holme and an anonymous referee for reviewing this article. This work was supported by the Leverhulme Trust.

REFERENCES

Alfvén, H., 1942. On the existence of electromagnetic—hydromagnetic waves, *Arkiv. Mat. Astron. Fys.,* **29B(2),** 1–7.

Allan, D.W. & Bullard, E.C., 1966. The secular variation of the Earth's magnetic field, *Proc. Camb. Phil. Soc.,* **62,** 783–809.

Backus, G.E., 1968. Kinematics of geomagnetic secular variation in a perfectly conducting core, *Phil. Trans. R. Soc. Lond.,* A, **263,** 239–266.

Bloxham, J. & Gubbins, D., 1985. The secular variation of the Earth's magnetic field, *Nature,* **317,** 777–781.

Bloxham, J. & Gubbins, D., 1986. Geomagnetic field analysis IV: testing the frozen-flux hypothesis, *Geophys. J. R. astr. Soc.,* **84,** 139–152.

Bloxham, J., 1988. The determination of fluid flow at the core surface from geomagnetic observations, in *Mathematical Geophysics, A Survey of Recent Developments in Seismology and Geodynamics,* pp. 189–208, eds Vlaar, N.J., Nolet, G., Wortel, M.J.R. & Cloetingh, S.A.P.L., D. Reidel, Hingham, MA.

Bloxham, J. & Jackson, A., 1992. Time-dependent mapping of the magnetic field at the core-mantle boundary, *J. geophys. Res.,* **97,** 19 537–19 563.

Braginsky, S.I., 1984. Short-period geomagnetic secular variation, *Geophys. Astrophys. Fluid Dyn.,* **30,** 1–78.

Braginsky, S.I., 1991. Towards a realistic theory of the geodynamo, *Geophys. Astrophys. Fluid Dyn.,* **60,** 89–134.

Braginsky, S.I. & LeMouël, J.L., 1993. Two-scale model of a geomagnetic field variation, *Geophys. J. Int.,* **112,** 147–158.

Bullard, E.C., Freedman, C., Gellman, H. & Nixon, J., 1950. The westward drift of the Earth's magnetic field, *Phil. Trans. R. Soc. Lond.,* A, **243,** 67–92.

Bullard, E.C. & Gellman, H., 1954. Homogeneous dynamos and terrestrial magnetism, *Phil. Trans. R. Soc. Lond.,* A, **247,** 213–278.

Chauvin, A., Gillot, P.Y. & Bonhommet, N., 1991. Paleointensity of the Earth's magnetic field recorded by two late quaternary volcanic sequences at the island of La Réunion (Indian Ocean), *J. geophys. Res.,* **96,** 1981–2006.

Coe, R.S., Grommé, S. & Mankinen, E.A., 1978. Geomagnetic paleointensities from radiocarbon-dated lava flows on Hawaii and the question of the Pacific non-dipole low, *J. geophys. Res.,* **83,** 1740–1756.

Creer, K.M., Irving, E. & Runcorn, S.K., 1954. The direction of the geomagnetic field in remote epochs in Great Britain, *J. Geomag. Geoelectr.,* **6,** 163–168.

Elsasser, W.M., 1947. Induction effects in terrestrial magnetism: Part III. Electric modes, *Phys. Rev.,* **72,** 821–833.

Gire, C., LeMouël, J.L. & Madden, T., 1986. Motions at the core surface derived from SV data, *Geophys. J. R. astr. Soc.,* **84,** 1–29.

Gonzalez, S., Sherwood, G., Böhnel, H. & Schnepp, E., 1997. Palaeosecular variation in central Mexico over the last 30 000 years: the record from lavas, *Geophys. J. Int.,* **130,** 201–219.

Gubbins, D., 1973. Numerical solutions of the kinematic dynamo problem, *Phil. Trans. R. Soc. Lond.,* A, **274,** 493–521.

Gubbins, D. & Kelly, P., 1993. Persistent patterns in the geomagnetic field during the last 2.5 Myr, *Nature,* **365,** 829–832.

Gubbins, D. & Kelly, P., 1996. A difficulty with using the frozen flux hypothesis to find steady core motions, *Geophys. Res. Lett.,* **23,** 1825–1828.

Gubbins, D., 1996. A formalism for the inversion of geomagnetic data for core motions with diffusion, *Phys. Earth planet. Inter.,* **98,** 193–206.

Halley, E., 1692. An account of the cause of the change of the variation of the magnetical needle, with an hypothesis of the structure of the internal parts of the Earth, *Phil. Trans. R. Soc. Lond.,* A, **16,** 563–578.

Hide, R., 1967. Motions of the Earth's core and mantle, and variation of the main geomagnetic field, *Science,* **157,** 55–56.

Hide, R. & Stewartson, K., 1972. Hydromagnetic oscillations of the Earth's core, *Rev. Geophys.,* **10,** 579–598.

Hulot, G. & LeMouël, J.L., 1994. A statistical approach to the Earth's main magnetic field, *Phys. Earth planet. Inter.,* **82,** 167–183.

Jackson, A. & Bloxham, J., 1991. Mapping the fluid flow and shear near the core surface using the radial and horizontal components of the magnetic field, *Geophys. J. Int.,* **105,** 199–212.

Jault, D. & LeMouël, J.L., 1991. Physical properties at the top of the core and core surface motions, *Phys. Earth planet. Inter.,* **68,** 76–84.

Kahle, A.B., Vestine, E.H. & Ball, R.H., 1967. Estimated surface motions of the Earth's core, *J. geophys. Res.,* **72,** 1095–1108.

Kumar, S. & Roberts, P.H., 1975. A three-dimensional kinematic dynamo, *Proc. R. Soc. Lond.,* **344,** 235–258.

LeMouël, J.L., Gire, C. & Madden, T., 1985. Motions at core surface in the geostrophic approximation, *Phys. Earth planet. Inter.,* **39,** 270–287.

Lloyd, D.B. & Gubbins, D., 1990. Toroidal fluid motions at the top of the Earth's core, *Geophys. J. R. astr. Soc.,* **100,** 455–467.

Love, J.J. & Gubbins, D., 1996a. Dynamos driven by poloidal flow exist, *Geophys. Res. Lett.,* **23,** 857–860.

Love, J.J. & Gubbins, D., 1996b. Optimized kinematic dynamos, *Geophys. J. Int.,* **124,** 787–800.

Madden, T. & LeMouël, J.L., 1982. The recent secular variation and the motions at the core surface, *Phil. Trans. R. Soc. Lond.,* A, **306,** 271–280.

Mankinen, E.A. & Champion, D.E., 1993a. Latest Pleistocene and Holocene geomagnetic paleointensity on Hawaii, *Science,* **262,** 412–416.

Mankinen, E.A. & Champion, D.E., 1993b. Broad trends in geomagnetic paleointensity on Hawaii during Holocene time, *J. geophys. Res.,* **98,** 7959–7976.

Opdyke, N.D. & Henry, K.W., 1969. A test of the dipole hypothesis, *Earth planet. Sci. Lett.,* **6,** 139–151.

Parker, E.N., 1963. Kinematical hydromagnetic theory and its application to the low solar photosphere, *Astrophys. J.,* **138,** 552–575.

Roberts, P.H. & Scott, S., 1965. On the analysis of the secular variation, *J. Geomag. Geoelectr.,* **17,** 137–151.

Rolph, T.C. & Shaw, J., 1986. Variations of the geomagnetic field in Sicily, *J. Geomag. Geoelectr.,* **38,** 1269–1277.

Roperch, P., Bonhommet, N. & Levi, S., 1988. Paleointensity of the Earth's magnetic field during the Laschamp excursion and its geomagnetic implications, *Earth planet. Sci. Lett.,* **88,** 209–219.

Salis, J.S., Bonhommet, N. & Levi, S., 1989. Paleointensity of the geomagnetic field from dated lavas of the Chaîne des Puys, France 1.7–12 thousand years before present, *J. geophys. Res.,* **94,** 15 771–15 784.

Steenbeck, M., Krause, F. & Rädler, K.H., 1966. Berechnung der mittleren Lorentz-Feldstärke $\overline{\mathbf{u}\times\mathbf{B}}$ für ein elektrisch leitendes Medium in turbulenter, durch Coriolis-Kräfte beeinflußter Bewegung, *Z. Naturforsch.,* **21a,** 369–376.

Tanaka, H., 1982. Geomagnetic paleointensities for the period 6000 to 3000 years B.P. determined from lavas and pyroclastic flows in Japan, *J. Geomag. Geoelectr.,* **34,** 601–617.

Tanaka, H., 1990. Paleointensity high at 9000 years ago from volcanic rocks in Japan, *J. geophys. Res.,* **95,** 17 517–17 531.

Tanaka, H., Otsuka, A., Tachibana, T. & Kono, M., 1994. Paleointensities for 10–22 ka from volcanic rocks in Japan and New Zealand, *Earth planet. Sci. Lett.,* **122,** 29–42.

Tanaka, H., Kawamura, K., Nagao, K. & Houghton, B.F., 1997. K-Ar ages and paleosecular variation of direction and intensity from Quaternary lava sequences in the Ruapehu Volcano, New Zealand, *J. Geomag. Geoelectr.,* **49,** 587–599.

Voorhies, C.V., 1986. Steady flow at the top of the Earth's core derived from geomagnetic field models, *J. geophys. Res.,* **91,** 12 444–12 466.

Voorhies, C.V., 1993. Geomagnetic estimates of steady surficial core flow and flux diffusion: unexpected geodynamo experiments, in *Dynamics of Earth's Deep Interior and Earth Rotation,* pp. 113–125, eds LeMouël, J.L., Smylie, D. & Herring, T., AGU Geophysical Monograph 72, IUGG Vol. 12.

Whaler, K.A. & Clarke, S.O., 1988. A steady velocity field at the top of the Earth's core in the frozen-flux approximation, *Geophys. J.,* **94,** 143–155.

Yukutake, T. & Tachinaka, H., 1969. Separation of the Earth's magnetic field into the drifting and standing parts, *Bull. Earthq. Res. Inst. Univ. Tokyo,* **47,** 65–97.

APPENDIX A: DETAILS OF DYNAMO CALCULATIONS

Method

Here we discuss the technical details of the kinematic dynamo calculations presented in Figs 5 and 6. The modelled system consists of an electrically conducting incompressible fluid sphere of unit radius surrounded by a solid electrical insulator. For such a system it is natural to adopt spherical coordinates (r, θ, ϕ). The (non-dimensionalized) induction equation

$$\partial_t \mathbf{B} = R_{\mathrm{m}}^{\mathrm{c}} \nabla\times(\mathbf{u}\times\mathbf{B}) + \nabla^2\mathbf{B} \tag{A1}$$

is solved by the Bullard & Gellman (1954) method: discretizing the equation by expanding both the magnetic field and flow in terms of toroidal and poloidal vector harmonics and radial grid points. We reduce the number of terms in the spherical harmonic expansion by a factor of four by requiring that the permissible solutions be antisymmetric under reflection through the equatorial plane and symmetric under azimuthal rotation by π radians. For a prescribed flow, $\mathbf{u}$, the induction equation is then reduced to an algebraic eigenvalue problem. Standard numerical techniques are used to solve for the magnetic field, $\mathbf{B}$, and the critical magnetic Reynolds number, $R_{\mathrm{m}}^{\mathrm{c}}$, at which dynamo action occurs. $R_{\mathrm{m}}^{\mathrm{c}}$ is defined after normalizing the flow so that $\langle\mathbf{u}\rangle = 1$, where $\langle\cdots\rangle$ denotes a volumetric rms average.

For clarity of notation we summarize briefly the mathematics. The magnetic field is the sum of toroidal and poloidal parts,

$$\mathbf{B} = \mathbf{T} + \mathbf{S}, \tag{A2}$$

where

$$\mathbf{T} = \nabla\times(T\hat{\mathbf{r}}), \quad \mathbf{S} = \nabla\times\nabla\times(S\hat{\mathbf{r}}). \tag{A3}$$

The dimensionless current density (given by Ampére's law in pre-Maxwell form) is just

$$\mathbf{J} = \nabla\times\mathbf{B}, \tag{A4}$$

and since

$$\nabla\times\mathbf{T} = \nabla\times\nabla\times(T\hat{\mathbf{r}}), \quad \nabla\times\mathbf{S} = \nabla\times[(-\nabla^2 S)\hat{\mathbf{r}}], \tag{A5}$$

we see that toroidal fields are sustained by poloidal currents and vice versa. The field is required to be analytical at the origin ($r = 0$), as well as match onto a potential field at the fluid surface ($r = 1$), where

$$\mathbf{B} = -\nabla\Phi. \tag{A6}$$

With no external sources the scalar function is described by an expansion in terms of Gauss coefficients g_l^m,

$$\Phi = a\sum_{l,m} g_l^m \left(\frac{a}{r}\right)^{l+1} Y_l^m. \tag{A7}$$

The spherical harmonics are

$$Y_l^{m\{c,s\}} = P_l^m \begin{Bmatrix} \cos m\phi \\ \sin m\phi \end{Bmatrix}, \tag{A8}$$

where $P_l^m(\cos\theta)$ is a Schmidt-normalized associated Legendre function of degree l and order m.

The flows considered here have surface characteristics we are interested in investigating in the context of testing the frozen-flux approximation; other than this, and the fact that they support dynamo action, they are rather arbitrary. The flows that sustain the dynamo models are modifications of that used by Kumar & Roberts (1975):

$$\mathbf{u} = \mathbf{t}_1^0 + \mathbf{s}_2^0 + \mathbf{s}_2^{2s} + \mathbf{s}_2^{2c}, \tag{A9}$$

where $\mathbf{b}$ and $\mathbf{s}$ are toroidal and poloidal vectors. The toroidal motion is differential rotation, whilst the poloidal motion is meridional plus multicellular convective overturning (details are given below). The flows are free-slip and non-penetrative at the surface ($r = 1$) and analytical at the origin ($r = 0$).

For dynamo 1 the scalar functions are

$$t_1^0 = \omega[br^2(1-r^2) + r(1-r)\sin(\pi r/2)], \tag{A10}$$

where

$$b = \frac{1}{\pi^5}(70\pi^3 - 5040\pi + 13440), \tag{A11}$$

and

$$s_2^0 = \alpha^0 r^6(1-r^2)^3, \tag{A12}$$

$$s_2^{2s} = \alpha^s[r^4(1-r^2)^2 - r^{12}\cos(\pi r/2)]\sin(3\pi r), \tag{A13}$$

$$s_2^{2c} = \alpha^c[r^4(1-r^2)^2 - r^{12}\cos(\pi r/2)]\cos(3\pi r). \tag{A14}$$

The surface flow is purely poloidal. The scalars $(\omega, \alpha^0, \alpha^s, \alpha^c)$ allow for the adjustment of the relative contribution of the different velocity ingredients. We find steady dynamo action for a flow with a large amount of poloidal motion; details are

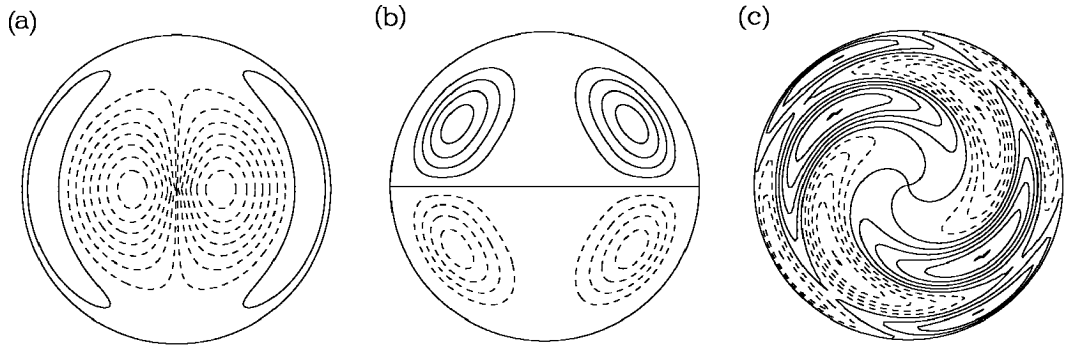

Figure A1. Velocity field for dynamo 1 given by eqs (A10)–(A14). (a) Meridional cross-section showing contours of toroidal flow t_ϕ. (b) Meridional cross-section showing streamlines of axisymmetric poloidal flow $\mathbf{s}_2^0$. (c) Equatorial cross-section showing streamlines of non-axisymmetric convective poloidal flow $\mathbf{s}_2^2$. Note that the convective flow is non-zero at the surface ($r=1$). Units are arbitrary with contour levels the same (for corresponding quantities) as in Fig. A2.

given in Table 2. Cross-sections of the fluid sphere showing the different velocity components are given in Fig. A1.

For dynamo 2 the scalar functions are

$$t_1^0 = \omega[br^2(1-r^2) + r\sin(\pi r/2)], \tag{A15}$$

where

$$b = \frac{1}{4\pi^4}(7\pi^4 - 840\pi^2 + 6720), \tag{A16}$$

and

$$s_2^0 = \alpha^0 r^6 (1-r^2)^3, \tag{A17}$$

$$s_2^{2s} = \alpha^s r^4 (1-r^2)^2 \sin(3\pi r), \tag{A18}$$

$$s_2^{2c} = \alpha^c r^4 (1-r^2)^2 \cos(3\pi r). \tag{A19}$$

The surface flow is purely toroidal. As with dynamo 1, the scalars (ω, α^0, α^s, α^c) allow for the adjustment of the relative contribution of the different velocity ingredients. We find steady dynamo action for a flow that is dominated by toroidal differential rotation; details are given in Table 2. Cross-sections of the fluid sphere showing the different velocity components are given in Fig. A2.

It is not always recognized that many steady kinematic dynamos have velocity fields with non-trivial angular momentum. With a steady dynamo solution in hand it is possible to transform to a reference frame fixed to the angular momentum of the flow by adding a solid-body rotation to an otherwise time-independent flow (the induction equation is rotationally invariant):

$$\mathbf{u} \rightarrow \mathbf{u} + \lambda \nabla \times (r^2 Y_1^0 \hat{r}), \tag{A20}$$

where the scalar λ fixes the angular velocity. The result of such a transformation is a steadily drifting magnetic field. For dynamo 1 the angular momentum of the prescribed flow (A10)–(A14) is zero, so no rotational transformation is made; on the other hand, for dynamo 2 the angular momentum is non-zero, so a transformation is desirable. To determine the appropriate drifting reference frame we first measure the angular momentum of our prescribed velocity field (A15)–(A19) in a frame fixed to the (steady) magnetic field:

$$\int u_\phi r \sin\theta dV = \omega \frac{4\pi}{15}; \tag{A21}$$

note that the poloidal flow contributes nothing to the angular momentum. For a solid-body rotation,

$$\lambda \int \nabla \times (r^2 Y_1^0 \hat{r})|_\phi \, r \sin\theta dV = \lambda \frac{8\pi}{15}. \tag{A22}$$

Thus, the shift to a reference frame corotating with the net angular momentum of the flow is given by

$$\lambda = -\frac{1}{2}\omega. \tag{A23}$$

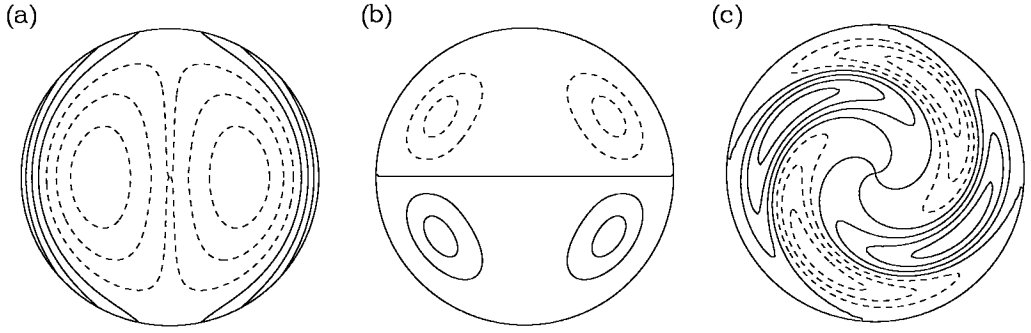

Figure A2. Velocity field for dynamo 2 given by equations (A15)–(A19). (a) Meridional cross-section showing contours of toroidal flow t_ϕ. (b) Meridional cross-section showing streamlines of axisymmetric poloidal flow $\mathbf{s}_2^0$. (c) Equatorial cross-section showing streamlines of non-axisymmetric convective poloidal flow $\mathbf{s}_2^2$. Note that the toroidal flow is non-zero at the surface ($r=1$). All quantities are shown in a reference frame of zero angular momentum; units are arbitrary with contour levels the same (for corresponding quantities) as in Fig. A1.

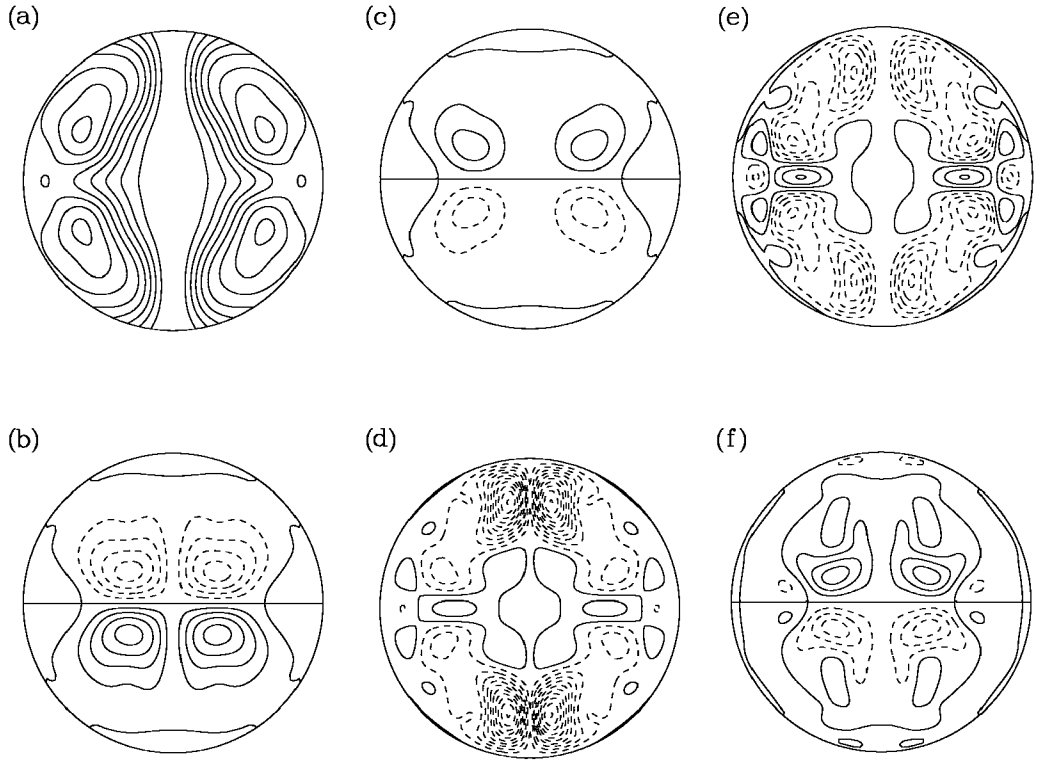

Figure A3. For dynamo 1, meridional cross-sections showing axisymmetric components of (a) poloidal magnetic field lines $\mathbf{B}_S$, (b) contours of B_ϕ, (c) lines of poloidal current density $\nabla \times \mathbf{T}$, (d) contours of J_ϕ, (e) lines of poloidal diffusion $\nabla^2\mathbf{S}$, (f) contours of $\nabla^2 B_\phi$. All units are arbitrary; contour levels are the same (for corresponding quantities) as in Fig. A4.

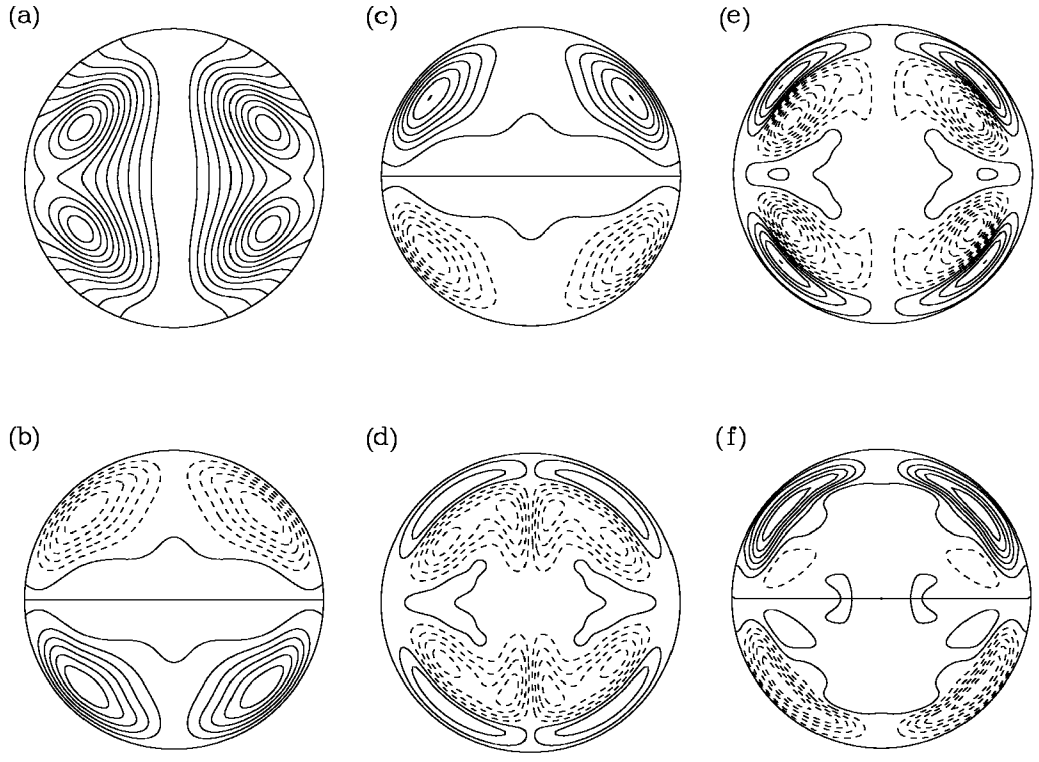

Figure A4. For dynamo 2, meridional cross-sections showing axisymmetric components of (a) poloidal magnetic field lines $\mathbf{B}_S$, (b) contours of B_ϕ, (c) lines of poloidal current density $\nabla \times \mathbf{T}$, (d) contours of J_ϕ, (e) lines of poloidal diffusion $\nabla^2\mathbf{S}$, (f) contours of $\nabla^2 B_\phi$. All units are arbitrary; contour levels are the same (for corresponding quantities) as in Fig. A3.

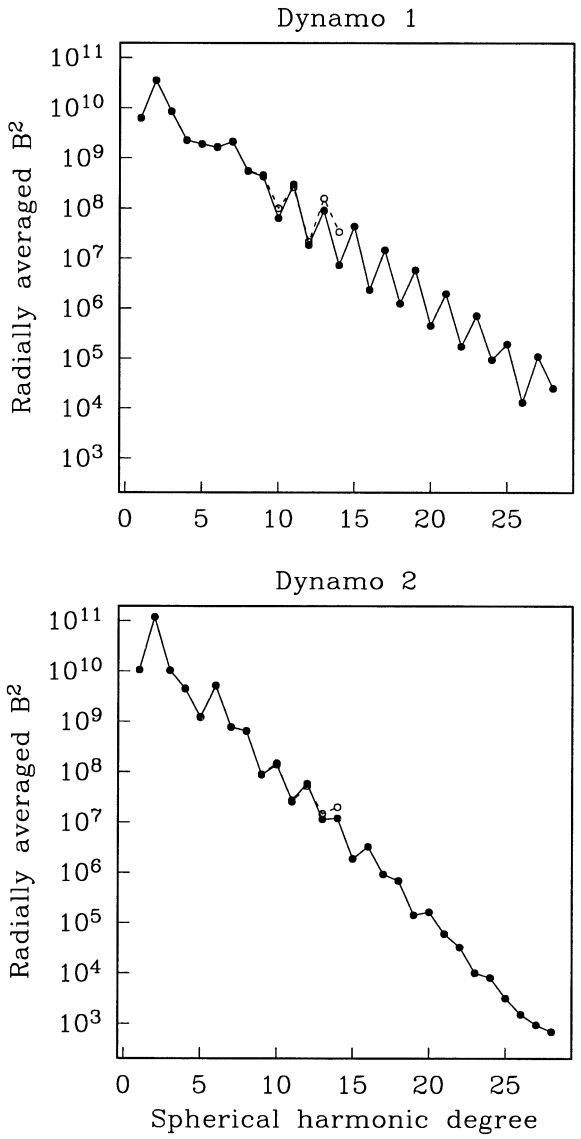

Figure A5. Magnetic energy (arbitrary units) as a function of spherical harmonic degree for dynamos 1 and 2. The dashed (solid) line represents the spectrum with spherical harmonic expansion truncated at degree 14 (28). The energy decreases with increasing harmonic degree, and since the models are adequately converged, the use of a higher-degree expansion would have little effect on the overall solution.

Such a transformation gives a time-dependent poloidal flow for dynamo 2 (in the reference frame corotating with the net angular momentum), but the toroidal flow, being axisymmetric, remains steady, and thus the surface flow of dynamo 2 is also steady after making the reference-frame transformation. If ω is positive (negative) we have a magnetic field drifting west (east), and a surface flow which is progressing at an equal rate but in the opposite eastward (westward) direction.

Model properties

Average properties of the models are given in Table 2; the axisymmetric components of the interior magnetic field, electric current and diffusion are shown in Figs A3 and A4. For both dynamos we find the familiar dominance of poloidal dipolar and toroidal quadrupolar magnetic fields, although in detail the arrangement of the fields is somewhat different for the two dynamos. Interestingly, the current density, as well as the diffusion, is distributed over the volume of the fluid; note, in particular, that there is no concentration of electrical current in a boundary layer, there is no current sheet, located just underneath the model core surface as has been postulated by Jault & LeMouël (1991). Clearly, the balance between diffusion and advection occurs over the volume of the fluid. In other words, the region just beneath the fluid surface is not qualitatively very different from the interior, although the details can vary depending on the particular flow.

Dynamo solutions must be checked to ensure that truncation of the spherical harmonic and radial gridpoint expansions is not made so prematurely that numerical convergence is not obtained. The usual procedure is to compare the solution at one truncation level with the solution obtained at a higher truncation level. If after successive increases in truncation the model is unchanged to within a numerically small and tolerable amount, then the result may be judged to be convergent (Gubbins 1973). In practice, checking for numerical convergence can require a substantial amount of computer power and for this reason apparently valid results can sometimes be illusive. In Fig. A5 we show the magnetic energy spectra for two different truncations of the spherical harmonics; the minor differences in the two spectra are indicative of a high degree of numerical convergence.